

Where do heavy particles go in a turbulent flow?

Mathieu Gibert^{1,4,*}, Haitao Xu^{1,4,†} and Eberhard Bodenschatz^{1,2,3,4‡}

¹Max Planck Institute for Dynamics and Self Organization, D-37073 Göttingen, Germany

²Institute for Nonlinear Dynamics, University of Göttingen, D-37073 Göttingen, Germany

³Laboratory of Atomic and Solid-State Physics and Sibley School of Mechanical and Aerospace Engineering, Cornell University, Ithaca, New York 14853 and

⁴International Collaboration for Turbulence Research

(Dated: March 3, 2019)

We report experimental results on the dynamics of heavy Kolmogorov-size particles in a fully developed turbulent flow. The mixed Eulerian structure function of two particle velocity and acceleration difference vector $\langle \delta_r \mathbf{v} \cdot \delta_r \mathbf{a}_p \rangle$ was observed to increase significantly with the particle inertia. We show that this increase can be attributed to a preferential alignment between these dynamical quantities. With increasing particle density the probability for those two vectors to be collinear was observed to grow. We show that this is a consequence of the fact that the inertial particles sample preferentially strain-dominated regions of the flow. This work opens a new approach towards a better understanding of the dynamics of the particle-turbulence interaction.

PACS numbers: 47.27.Gs, 47.27.Jv, 47.80.Cb

Turbulence occurs whenever fluid viscous forces are small compared to the dominant driving forces of the flow. In practice this includes most macroscopic natural and technological flows. Very frequently, these turbulent flows are loaded with passive particles with non-negligible inertia, i.e., particles do not exactly follow fluid motion. Familiar examples of such flows include the clouds in the atmosphere, sand storms in arid regions, pneumatic transports of grains in pharmaceutical and food industries, fluidized beds in chemical engineering, and fuel sprays in combustion engines and turbines. The understanding of particle-turbulence interaction is therefore of central importance to our ability to make advances in key economical and societal issues like energy generation, climate change, and pollution control. Comparing to the fluid turbulence problem itself, which is well described by the non-linear Navier-Stokes equations, the particle-turbulence interaction problem is on a much weaker foundation. In principle, the particle dynamics can be obtained by solving particle equations coupled with the Navier-Stokes equations for the fluid with no-slip boundary conditions on particle surfaces. However, this approach is a formidable task for theoretical and numerical investigations [1, 2]. Most theoretical analyses and numerical simulations therefore must rely on simplified equations, in which the particle-turbulence interactions are modeled. An interesting result obtained from these simplified equations is that in a turbulent flow particles with small to moderate inertia tend to move to regions with high strain and low vorticity [3]. This so-called “preferential concentration” of inertia particles is under intensive investigation [4–9] and has been invoked when studying droplet collision rates in warm clouds [10, 11] and plankton encounter rates in ocean [12]. Inhomogeneous distributions of inertial particles in turbulent flows have also been observed in several experiments [13–16]. However, experimental evidences that the high particle

concentration regions are also high-strain/low-vorticity regions are still elusive. A step forward is achieved in a recent experiment which reported that the velocity fields averaged around large particles, slightly heavier than fluid, were strain-dominated [17].

In this Letter, we report experimental measurements of particle motions in a fully developed turbulent water flow. The solid spherical particles have the same average sizes, but their densities vary between $1 \lesssim \rho_p/\rho_f \lesssim 8$, where ρ_p and ρ_f are particle and fluid densities, respectively. So far, scientists used the time averaged radial distribution function of inertial particles to probe the preferential concentration effect. We propose that this effect may be better captured by the *dynamical* variables since preferential concentration is a direct consequence of particle dynamics. The relative velocities $\delta_r \mathbf{v}$ and the relative accelerations $\delta_r \mathbf{a}_p$ between two inertial particles are particularly well suited. We show that the statistics of the angle between $\delta_r \mathbf{v}$ and $\delta_r \mathbf{a}_p$ change significantly with particle density. A comparison with a linear velocity gradient model suggests that this change is associated with the accumulation of inertial particles in strain-dominated regions of the turbulent flow field. Our approach therefore opens a new way to study particle-turbulence interaction.

We carried out three-dimensional Lagrangian Particle Tracking measurements [18, 19] to obtain the trajectories of solid particles with different densities in a turbulent water flow. The experiment is described in detail in [20]. We give here a brief summary. The turbulent flow was generated by two counter-rotating baffled disks in a hexagonal shaped water chamber. The axis of rotation of the disks was in the horizontal direction so that the heavy particles settling down towards the bottom of the apparatus were entrained by the strong sweeping of the fluid near the surface. In this way particles stayed longer suspended in the fluid. The spherical measure-

	ρ_p/ρ_f	d_p (μm)	d_p/η	St
Polystyrene	1.06	74 ± 10	0.98	0.08
Glass	4	75 ± 8	1.04	0.24
Steel	7.8	75 ± 15	1.04	0.44

TABLE I: Characteristics of the different particles used in the experiments. The Stokes number was defined as $St \equiv d_p^2/12\beta\eta^2$, where d_p is the particle diameter, $\beta \equiv 3\rho_f/(2\rho_p + \rho_f)$ is the modified density ratio, that takes into account the added mass effect, and η is the Kolmogorov length scale of the turbulence.

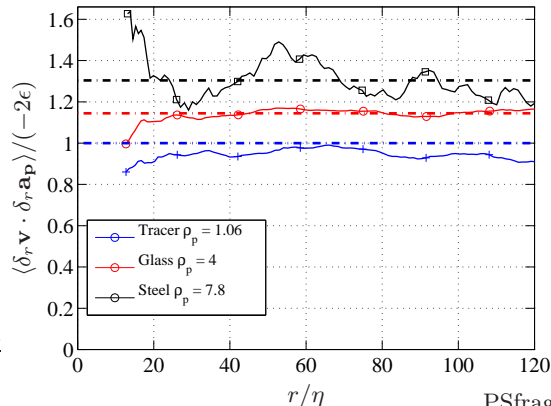
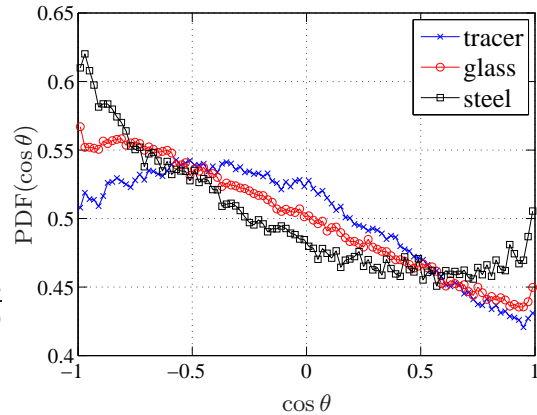


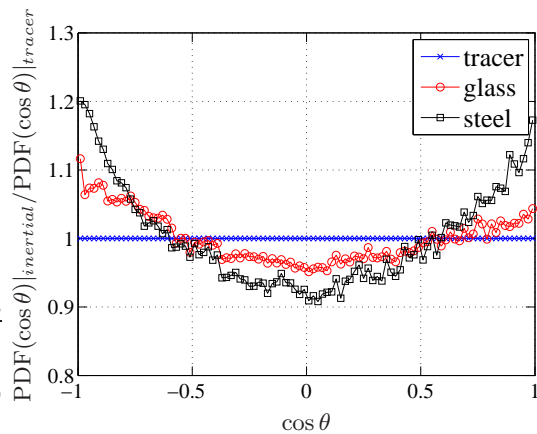
FIG. 1: Mixed Eulerian velocity-acceleration structure function $\langle \delta_r \mathbf{v} \cdot \delta_r \mathbf{a} \rangle$ normalized by the expected values for the fluid particles -2ϵ . The values of the different plateaus represented by the dot-dashed lines are : blue 1, red 1.15, black 1.30. The larger fluctuations in the data for the steel particles ($St \approx 0.5$) are due to less statistics. These steel particles had high settling velocity and moved out the measurement volume quickly.

ment volume with a diameter of 22 mm was located at the center of the water chamber, where the mean flow was small compared to the fluctuations. We used three different types of particles: polystyrene, glass, and stainless steel. These particles were of the same average size, but different densities within the range $1 \lesssim \rho_p/\rho_f \lesssim 8$. The Taylor microscale Reynolds number of the turbulent flow was $R_\lambda = 442$, at which the Kolmogorov scale η , the smallest scale in turbulence, was $74\ \mu\text{m}$, close to the particle size: $d_p/\eta \approx 1$. The resulting Stokes numbers (see Table I) were between 0.08 and 0.5. The particles properties are summarized in table I. The spatial resolution of $45\ \mu\text{m}$ per pixel and the temporal resolution of 31 frames per Kolmogorov time τ_η were high enough for us to accurately measure particle velocity and acceleration [21].

With the measured particle trajectories, we studied the turbulent relative dispersion of inertial particles. We observed an increase of relative velocity with particle den-



(a)



(b)

FIG. 2: (a) Probability density function of the cosine of the angle θ between $\delta_r \mathbf{v}$ and $\delta_r \mathbf{a}_p$ for the three types of particles for a separation $r/\eta = 28 \pm 7$. (b) Same PDFs as in (a) normalized by the tracer particles one. This figure shows the relative effect of the particle inertia on the alignment/anti-alignment of $\delta_r \mathbf{v}$ with $\delta_r \mathbf{a}_p$.

sity. As a consequence, heavier particles separated from each other faster than fluid tracers at the early stage of relative dispersion [20]. When analysing the dynamics of these heavy particles, we noticed a strong effect of particle density on the mixed velocity-acceleration Eulerian structure function $\langle \delta_r \mathbf{v} \cdot \delta_r \mathbf{a}_p \rangle$, where $\delta_r \mathbf{v}$ and $\delta_r \mathbf{a}_p$ are the relative velocity and the relative acceleration between two particles separated at distance r . For fluid turbulence, it has been shown [22–25] that in the inertial range, this mixed structure function equals a constant: $\langle \delta_r \mathbf{u} \cdot \delta_r \mathbf{a} \rangle = -2\epsilon$, where \mathbf{u} and \mathbf{a} are fluid velocity and acceleration, respectively. In our experiments, the polystyrene particles behaved as tracer particles and the energy dissipation rate ϵ measured using the equation above agreed well with the value obtained from other methods [20]. As shown in Figure 1, for inertial parti-

cles, this mixed velocity-acceleration structure functions in the inertial range were still constant, but the values increased significantly by 30% when the particle Stokes number increased from 0.06 to 0.5. The observed change in $\langle \delta_r \mathbf{v} \cdot \delta_r \mathbf{a}_p \rangle$ cannot be explained by only the changes in the magnitudes of $\delta_r \mathbf{v}$ and $\delta_r \mathbf{a}_p$. The reason lies in the alignment between these two vectors, measured by the cosines of the angle θ between the two:

$$\cos \theta = \frac{\delta_r \mathbf{v} \cdot \delta_r \mathbf{a}_p}{|\delta_r \mathbf{v}| |\delta_r \mathbf{a}_p|}. \quad (1)$$

The effect of particle inertia on $\cos \theta$ is best demonstrated by its probability density function (PDF). Figure 2a shows the PDFs of $\cos \theta$ corresponding to $\delta_r \mathbf{v}$ and $\delta_r \mathbf{a}_p$ at separation $r = (28 \pm 7)\eta$ for the three different particles we measured. Qualitatively similar effect were observed at other separations r . All these PDFs are skewed to the side of $\cos \theta < 0$, i.e., the two vectors are in opposite directions. The skewness increases with particle inertia. These observations are consistent with the increase (in absolute value) of $\langle \delta_r \mathbf{v} \cdot \delta_r \mathbf{a}_p \rangle$ shown in Figure 1.

To better understand the relative effect of particle inertia, we plot in Figure 2b the PDFs of the two inertial particles normalized by the PDF of the fluid tracers. Clearly, the particle inertia enhanced the collinearity, either in the same direction or in the completely opposite direction, between relative velocity and relative acceleration vectors. The PDFs are slightly skewed toward the anti-alignment side ($\cos \theta < 0$). For this range of Stokes number, as shown numerically and experimentally in [20, 26], at the particle position the difference between particle acceleration and that of the fluid is negligible as far as the dynamical variables $\delta_r \mathbf{a}_p$ and $\delta_r \mathbf{v}$ are concerned. If the inertial particles were homogeneously distributed in space, like fluid tracers, we would not observe any differences between the PDFs of fluid tracers and inertial particles. Therefore, our measurements show that inertial particles preferentially explore certain regions of the flow, leading to the observed PDFs in Figure 2. To further understand which features of the flow are responsible for the observed behaviour, we investigate $\delta_r \mathbf{u}$ and $\delta_r \mathbf{a}$ of fluid tracers for particular flow fields.

Lets consider a steady, incompressible linear velocity field u_i defined by :

$$u_i = M_{ij} x_j \quad (2)$$

where u_i is the fluid velocity at position x_i , M_{ij} is the velocity gradient tensor. In our experiments, where the separation r are in the inertial range, we should treat M_{ij} as a coarse-grained velocity gradient at scale r [27]. For a steady flow, the fluid acceleration field a_i is also determined by M_{ij} : $a_i = u_j \frac{\partial u_i}{\partial x_j} = M_{ik} M_{kj} x_j$. For a velocity field with pure rotation, the fluid acceleration is always normal to its velocity, i.e., $\delta_r \mathbf{a} \cdot \delta_r \mathbf{u} = 0$. The PDF

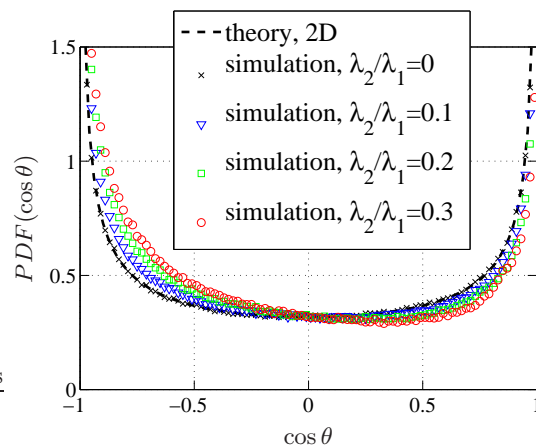


FIG. 3: PDF of the same quantity considered in figure 2 inset, obtained in the case of fluid particles evolving in a steady linear purely strained flow. The different curves correspond to different ratios of λ_2/λ_1 (see legend).

of $\cos \theta$ is a δ -function at $\cos \theta = 0$. This is not consistent with our observations.

For a pure straining velocity field, the three eigenvalues of M_{ij} are all real and can be arranged as $\lambda_1 \geq \lambda_2 \geq \lambda_3$. Incompressibility requires that $\lambda_1 + \lambda_2 + \lambda_3 = 0$. It is straightforward to show that the alignment between relative velocity and relative acceleration vectors depends only on the orientation of the separation vector \mathbf{r} between the two particles and λ_2/λ_1 . The PDF of $\cos \theta$ is then obtained by assuming that \mathbf{r} distributes uniformly in all directions. When $\lambda_2 = 0$, i.e., the two-dimensional case, the PDF is:

$$PDF(\cos \theta) = \frac{1}{\pi(1 - \cos^2 \theta)^{1/2}}. \quad (3)$$

For $\lambda_2/\lambda_1 \neq 0$, the PDFs are obtained numerically. For $\lambda_2/\lambda_1 = 0$, the numerical simulation agrees with our analytical solution. It is well known that in turbulent flows the average of the eigenvalue ratio of velocity gradient is positive, with a value of $\langle \lambda_2/\lambda_1 \rangle \approx 0.15$ [28–32]. We therefore performed simulations with the range of λ_2/λ_1 around this value. Figure 3 shows the PDFs of $\cos \theta$ from the simulation results with $0 \leq \lambda_2/\lambda_1 \leq 0.3$, together with the analytical solution Eq. (3). The PDFs for $\lambda_2/\lambda_1 > 0$ in Fig. 3 are remarkably similar to the “relative PDFs” shown in Figure 2b, namely, the relative accelerations and the relative velocities prefer to be collinear, with slight skewness to the anti-alignment side. This observation, together with the fact that inertial particles have to leading order, the velocities and accelerations of the fluid [20, 26], suggests that inertial particles sample preferentially strain-dominated regions in turbulence. Our approach should be compared with results from numerical simulations of simplified equations, for which the phenomenon of “preferen-

tial sampling of strain-dominated regions” has been observed [6, 7]. There the velocity fields around the virtual inertial point particles was investigated. It will be interesting to see how well the PDFs of $\cos\theta$ agree with the experimental results presented here. Moreover, studying the PDF of $\cos\theta$ for fluid tracers might reveal new information about the structures of the turbulent flow itself, e.g., by conditioning of the PDF on local strain rates and vorticities.

In summary, we have observed a very significant increase of the mixed structure function $\langle\delta_r\mathbf{v}\cdot\delta_r\mathbf{a}_p\rangle$ when increasing the density of Kolmogorov-size particles. We found that this increase could not be attributed to the magnitudes, but the angle between the relative velocity and relative acceleration. By analogy to a linear pure straining flow, we were able to show that heavy particles preferentially explore strain-dominated regions of a turbulent flow. This effect is well quantified by the PDF of the cosine of the angle between the relative velocity and acceleration vectors of heavy particles normalized by that of tracers. The tendency of heavy particles to preferentially explore strain-dominated regions may also explain our recent observations [33] that the average, radial, Eulerian particle density distribution function shows an increase when the center of the von Kármán flow is approached. In this case, the system has in average a strong strain dominated region and, with the observations above, one would expect that deterministically the long time average would lead to a measurable preferential concentration with respect to the center of the apparatus. Our analysis has the advantage, that it does not rely on the long time average of the relative positions of particles, but rather captures quantitatively the dynamical properties. Our approach therefore opens novel ways to study particle-turbulence interaction. For higher Stokes number, the filtering induced by the particle response time [26] will have an additional effect on the analysis presented above. To go beyond this experimental approach, simultaneous measurements of inertial particle trajectories and the spatio/temporally resolved flow field around are needed. This will be the focus of future investigations.

We acknowledge R. J. Hill, A. Pumir and E. -W. Saw for many interesting discussions. This work was funded by the Max Planck Society, and the Marie Curie Fellowship, Programme PEOPLE - Call FP7-PEOPLE-IEF-2008 Proposal N° 237521.

* Electronic address: mathieu.gibert@ds.mpg.de

† Electronic address: haitao.xu@ds.mpg.de

- ‡ Electronic address: eberhard.bodenschatz@ds.mpg.de
- [1] J. Happel and H. Brenner, *Low Reynolds Number Hydrodynamics* (Prentice-Hall, 1965).
 - [2] H. Homann and J. Bec, *J. Fluid Mech.* **Submitted**, [arXiv:0909.5628](#) (2009).
 - [3] M. Maxey and J. Riley, *Phys. Fluids* **26**, 883 (1983).
 - [4] G. Falkovich and A. Pumir, *Phys. Fluids* **16**, L47 (2004).
 - [5] L. I. Zaichik and V. M. Alipchenkov, *New J. Phys.* **11**, 103018 (2009).
 - [6] J. Chun, D. Koch, S. Rani, A. Ahluwalia, and L. Collins, *J. Fluid Mech.* **536**, 219 (2005).
 - [7] L. Collins and A. Keswani, *New J. Phys.* **6**, 119 (2004).
 - [8] S. Sundaram and L. Collins, *J. Fluid. Mech.* **335**, 75 (1997).
 - [9] L. Ducasse and A. Pumir, *Phys. Rev. E* **77**, 066304 (2008).
 - [10] J. Shaw, *Ann. Rev. Fluid Mech.* **35**, 183 (2003).
 - [11] G. Falkovich, A. Fouxon, and M. G. Stepanov, *Nature* **419**, 151 (2002).
 - [12] F. C. Schmitt and L. Seuront, *J. Mar. Sys.* **70**, 263 (2008).
 - [13] A. Aliseda, A. Cartellier, F. Hainaux, and J. Lasheras, *J. Fluid Mech.* **468**, 77 (2002).
 - [14] A. Wood, W. Hwang, and J. Eaton, *Int. J. Multiphas Flow* **31**, 1220 (2005).
 - [15] J. P. L. C. Salazar, J. D. Jong, L. Cao, S. H. Woodward, H. Meng, and L. R. Collins, *J. Fluid Mech.* **600**, 245 (2008).
 - [16] E. W. Saw, R. A. Shaw, S. Ayyalasomayajula, P. Y. Chuang, and A. Gylfason, *Phys. Rev. Lett.* **100**, 214501 (2008).
 - [17] M. Guala, A. Liberzon, K. Hoyer, A. Tsinober, and W. Kinzelbach, *J. Turbul.* **9**, 1 (2008).
 - [18] N. T. Ouellette, H. Xu, and E. Bodenschatz, *Exp. Fluids* **40**, 301 (2006).
 - [19] H. Xu, *Meas. Sci. Technol.* **19**, 075105 (2008).
 - [20] M. Gibert, H. Xu, and E. Bodenschatz., *Europhys. Lett.* **Submitted**, [arXiv:1002.1805](#) (2010).
 - [21] H. Xu, N. T. Ouellette, D. Vincenzi, and E. Bodenschatz, *Phys. Rev. Lett.* **99**, 204501 (2007).
 - [22] J. Mann, S. Ott, and J. Andersen, *Risø-R-1036(EN)* (1999).
 - [23] R. J. Hill, *J. Fluid Mech.* **434**, 379 (2001).
 - [24] G. Falkovich, K. Gawędzki, and M. Vergassola, *Rev. Mod. Phys.* **73**, 913 (2001).
 - [25] A. Pumir, B. Shraiman, and M. Chertkov, *Europhys. Lett.* **56**, 379 (2001).
 - [26] J. Bec et al., *J. Fluid Mech.* **550**, 349 (2006).
 - [27] M. Chertkov, A. Pumir, and B. Shraiman, *Physics of Fluids* **11**, 2394 (1999).
 - [28] R. Betchov, *J. Fluid Mech.* **1**, 497 (1956).
 - [29] W. T. Ashurst, A. R. Kerstein, R. M. Kerr, and C. H. Gibson, *Phys. Fluids* **30**, 2343 (1987).
 - [30] M. Kholmyansky, A. Tsinober, and S. Yorish, *Phys. Fluids* **13**, 311 (2001).
 - [31] B. Lüthi, A. Tsinober, and W. Kinzelbach, *J. Fluid Mech.* **528**, 87 (2005).
 - [32] J. Berg, B. Lüthi, J. Mann, and S. Ott, *Phys. Rev. E* **74**, 16304 (2006).
 - [33] H. Xu and E. Bodenschatz, *Physica D* (2008).